Effects of diagenesis on magnetic mineralogy in a Jurassic claystone-limestone succession from the Paris Basin

Marie Gabrielle Moreau, Magali Ader

JOURNAL OF GEOPHYSICAL RESEARCH, VOL. 105, NO. B2, PAGES 2797-2804, FEBRUARY 10, 2000

Effects of diagenesis on magnetic mineralogy in a Jurassic claystone-limestone succession from the Paris Basin

Marie Gabrielle Moreau

Laboratoire de Paléomagnétisme, Institut de Physique du Globe de Paris, Paris, France

Magali Ader

Laboratoire de Géochimie des Isotopes Stables, Institut de Physique du Globe de Paris, Paris, France

Abstract. We performed detailed rock magnetic and geochemical analyses on a previously published Early Jurassic magnetostratigraphic section. The results improve our understanding of acquisition and preservation processes of magnetization in a series of alternating claystones and limestones. The main carrier of magnetization is magnetite. Anhysteretic remanent magnetization (ARM) varies by a factor of 40 and the ARM variations are linked to magnetite grain size. Comparison of magnetic and geochemical data shows that when carbonate content is high (>30%) and $\delta^{13}C \approx 0‰$, magnetite is characterized by small grain sizes, whereas when carbonate content is low (<20%), magnetite is coarse-grained. It appears that the oxidation of organic matter by sulfate reduction controls both $\delta^{13}C$ and magnetite grain size. H_2S produced during sulfate reduction causes partial dissolution of magnetite grains, with the finest magnetite grains (those that best record the magnetic signal) being dissolved first. Despite this partial dissolution, both the direction and polarity of the original remanent magnetization are preserved.

1. Introduction

McNish and Johnson [1938] studied the natural remanent magnetization (NRM) of marine sediments. Since that time, several authors [e.g., *Irving and Major*, 1964; *Collinson*, 1965; *Kent*, 1973; *Lund and Karlin*, 1990] have studied the physical, chemical, and biological processes that record the terrestrial magnetic field in marine or continental sediments. Studies on recent sediments are numerous and tend to suggest that the recording of the field depends on local physical and chemical conditions at the time of sedimentation. Within the first few decimeters of burial, it is possible to create and to dissolve magnetic carriers [*Leslie et al.*, 1990; *Karlin*, 1990; *Channel and Hawthorne*, 1990; *van Hoof and Langereis*, 1991; *Schwartz et al.*, 1996]. While significant advances have been made in this field, the acquisition process of NRM remains insufficiently understood. In this paper, we investigate this process in a series of alternating claystones and limestones.

2. Choice of the Montcornet Section

A magnetostratigraphic section of Hettangian and Sinemurian sediments was previously reported by *Yang et al.* [1996] from a drill core obtained from the northern part of the Paris Basin. We have since measured the anhysteretic remanent magnetization (ARM) of these sediments in order to estimate the relative intensity changes of the terrestrial magnetic field during this period. The ARM exhibits rapid variations up to a factor of 40, while the weak field susceptibility varies by less than a factor of 5. We noticed that reversals defined by only one or two samples sometimes correlated with peaks in ARM intensity. These observations motivated us to further examine the acquisition of remanence in these sediments.

We focused on part of the core between 1020 and 1055 m depth (Figures 1a and 1b), where rapid variations in ARM intensity and reversal frequency are commonly defined by only one or two samples. This 35 m thick claystone-limestone succession was deposited in an intertidal marine environment, in a time span of 3 million years, at around 200 Ma. These rocks are mudstones composed of micrite, clay, and silt, in varying proportions, and contain small amounts of recrystallized bioclasts, coal debris, pyrite, and framboïdal pyrite. An isotopic study of this interval has being published separately [*Ader and Javoy*, 1998].

For the Montcornet section, *Yang et al.* [1996] showed that after removal of a recent overprint by thermal demagnetization to 300°C, alternating field demagnetization isolated the primary magnetic component. This hybrid demagnetization technique was successful because the carrier had low coercivities and was likely magnetite. Magnetic directions of the primary remanence of individual samples were always well defined. In the present study, we found that six samples have strong ARMs (>0.12 A/m) in a normal polarity zone, between 1052 and 1044 m. One of the six has a reversed direction. In a reversed zone (from 1026 to 1028 m), three samples have strong ARMs, two of which have normal polarities. The presence of dual polarities in these two zones excludes the possibility of a complete thermal remagnetization occurring during a single polarity event. This conclusion is further strengthened by the lack of geologic structures (deformation, volcanoes, etc.) indicative of thermal or tectonic activity in the vicinity.

We questioned whether the ARM variations are attributable to variations in the sediment lithology such as (1) detrital flux, (2) authigenesis of magnetic minerals, and/or (3) preservation of the

Paper number 1999JB900319.
0148-0227/00/1999JB900319$09.00

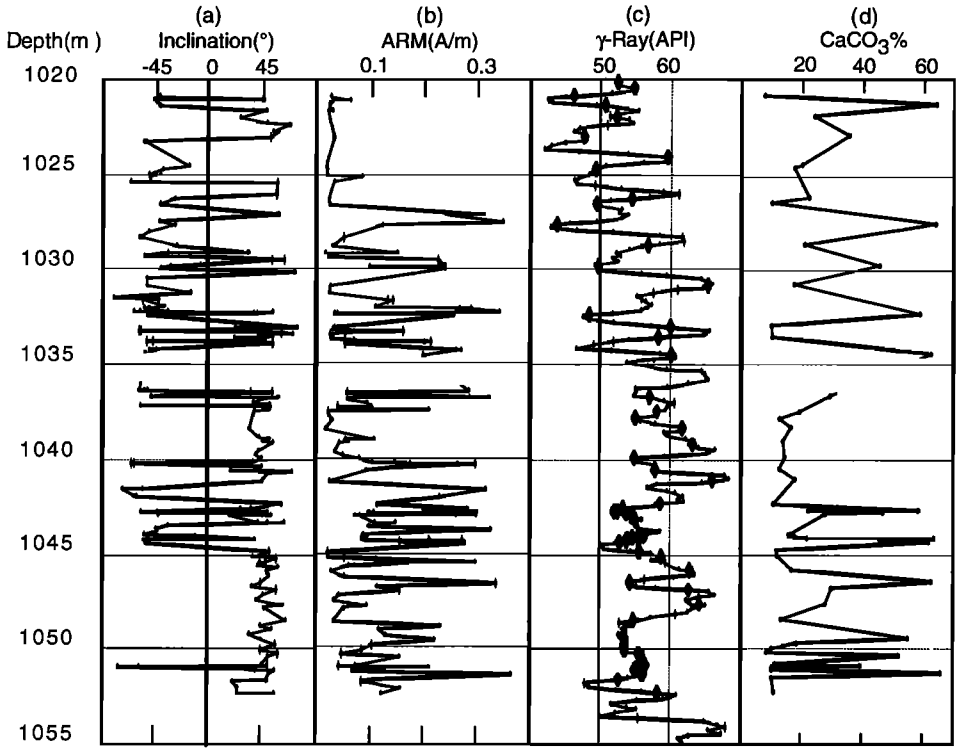

Figure 1. Variations versus depth: (a) inclination [after Yang et al., 1996], (b) ARM, (c) gamma-ray with samples plotted, (d) carbonate content [after *Ader and Javoy*, 1998].

magnetic phases during diagenesis. Moreover, what influences would these variations have on the magnetic field record?

3. Experimental Study

3.1. Microscopic study of magnetic fraction

We performed scanning electron microscopy (SEM) on magnetic separates. We separated the magnetic fractions as described below. Crushed samples were disintegrated via ultrasound in a distilled water bath. A rare earth magnet (placed in a thin-walled tube of latex rubber) was suspended in the mixture during the ultrasound treatment for about 5 min. The magnet was removed from the rubber tube, and the magnetic particles washed into a collecting dish. This procedure was repeated until no more magnetic particles could be retrieved from the original sample. We then performed SEM observations and chemical mapping to identify the mineralogy of the magnetic separates. They consisted of pure iron oxides (magnetite or hematite), iron and titanium oxides (titanomagnetite or titanohematite), and iron and chromium oxides (chromite). The proportions of chromium and titanium relative to iron vary, as is common in detritic sediments [*Dunlop and Özdemir*, 1997]. Grain shapes are irregular, and their sizes vary from approximately 1 μm to 30 μm. In carbonate-poor samples, coarse grains larger than 5 μm are strongly dominant, and magnetite and titanomagnetite grains show obvious etching and dissolution. In carbonate-rich samples, no dissolution was observed. Grains smaller than 5 μm are dominant, with the smallest observed fraction (0.3 to 1 μm) being essentially pure magnetite. For the latter samples, chemical mapping of carbonate-rich grain aggregates showed a significant level of dispersed iron. This iron is not associated with the usual clay constituents (Al, Si and K), and Ti and Cr are also absent. These chemical observations, along with the fact that these carbonate aggregates were attracted to the magnet lead us to propose that this iron lies within very fine magnetite grains.

3.2. Magnetic study

The 58 samples from the geochemical and magnetic study are plotted on the gamma-ray log in Figure 1c. These samples cover a wide range of lithologies and $CaCO_3$ contents. Seventeen of these 58 samples, which have ARM values between 0.01 and 0.5 A/m, were selected for a more comprehensive study of their magnetic properties. For these samples we studied the acquisition of ARM, the acquisition of isothermal remanent magnetization (IRM), the thermal demagnetization of the IRM, and the magnetic hysteresis. Figure 2 shows the results of these analyses for sample 1036.93 (left side, Figure 2a-2e), which possesses a relatively weak ARM, and for sample 1050.64 (right side, Figure 2f-2j), which possesses a relatively strong ARM.

ARM acquisition curves were traced in a continuous field of 0.1 mT while simultaneously applying an alternating field from 0 to 90 mT. Saturation is never reached in any of the samples, and the normalized acquisition curves are similar for all of the samples (e.g., Figure 2a, and 2f). Maximum ARM intensities vary from 0.01 to 0.4 A/m.

For some samples, IRM saturation was achieved at 0.1 T (Figure 2g), whereas for others, saturation did not occur in applied fields up to 1.2 T (Figure 2b). In the former case, the magnetic carrier possessed a weak coercivity and is probably magnetite. Maximum IRM intensities in 1.2 T applied fields vary between 0.2 and 2 A/m.

Following the method described by *Lowrie* [1990], a composite IRM was subsequently thermally demagnetized,

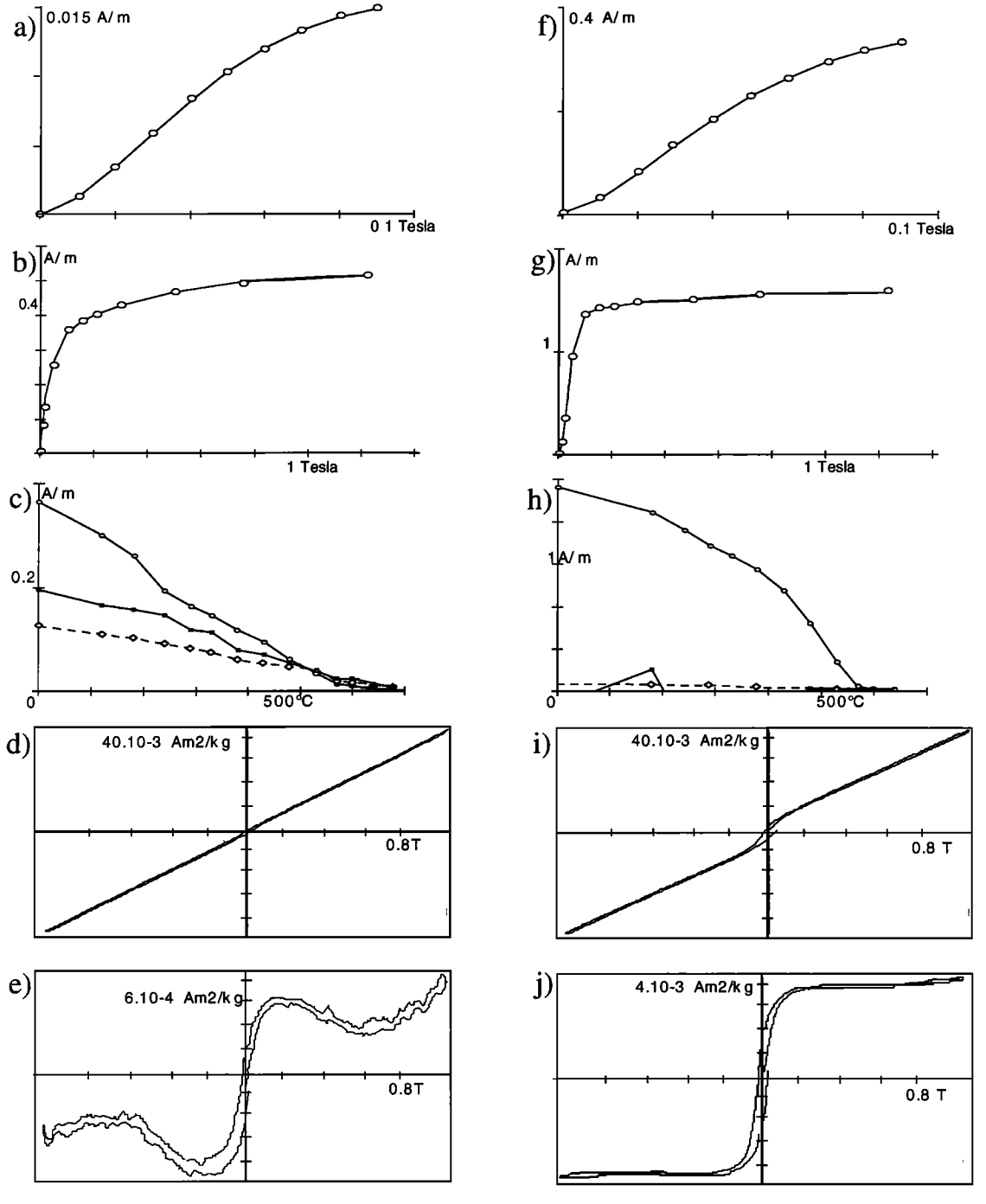

Figure 2. Examples from the rock magnetic analyses. Left column is sample 1036.93, which exhibits a weak ARM. Right column is sample 1050.64, which exhibits a strong ARM. (a and f) acquisition of ARM; (b and g) acquisition of IRM, and (c and h) stepwise thermal demagnetization of three-component IRM [*Lowrie*, 1990]. Circles indicate soft component (0.12 T), squares indicate medium component (0.4 T), and diamonds indicate hard component (1.2 T). In (h) the intensity of the soft component masks other components. (d and i) Hysteresis loop up to 1 T; (e and j) ferromagnetic hysteresis loop after subtracting the paramagnetic contribution. The loop in (e) is noisy, while that in (j) is well-defined.

allowing a more accurate identification of the magnetic carriers. Magnetic fields of 1.2, 0.4, and 0.12 T were successively applied to each of the three perpendicular sample axes prior to thermal demagnetization. The low blocking field component is dominant and usually corresponds to a maximum unblocking temperature of about 580°C (Figure 2c, and 2h), confirming that magnetite is the principal magnetic carrier. For samples with strong ARMs (in general >0.12 A/m), the demagnetization curves of the soft component is convex upward with a rapid decay between 400°C and 580°C (Figure h), which probably indicates the presence of fine-grained magnetite. For samples with weak ARMs (<0.12 A/m), the demagnetization curve of the soft component is linear

between 25°C and 580°C (Figure 2c). This likely indicates either the absence of fine magnetite grains or the presence of titanomagnetite. For all samples the hard and medium components indicate unblocking temperatures of 680°C, suggesting the presence of hematite. The presence of the hematite-bearing components is more prevalent in samples with weak ARMs, when the intensity of the soft component is weak. In such cases, 10 to 15% of the remanence likely resides in hematite.

Because the main magnetic carrier is magnetite, we measured the hysteresis parameters of the samples. The loops were traced to 1 T. A strong paramagnetic signal always obscures the ferromagnetic one (Figure 2d, and 2i) and is attributed to the presence of clay and pyrite [*Yang, et al.*, 1996]. High field susceptibility values range from 36 to 72 ($x10^{-9}$) m^3/kg. We tried to isolate the ferromagnetic component by subtracting the paramagnetic component (Figure 2j). If the paramagnetic signal represents more than 95% of the induced magnetization, the residual signal is blurred (Figure 2e), and it is very difficult to isolate the hematite contribution to magnetization in a strong field (some 0.5% of the total induced magnetization). Due to the dominance of the paramagnetic component, high-field hysteresis parameters are obscured and have very large errors (probably 100%).

3.3 Grain size of magnetite.

One approach to determine the grain size of magnetite, besides interpreting hysteresis parameters, is to compare the anhysteretic susceptibility with the weak field susceptibility [*King et al.*, 1982, 1983]. The Montcornet samples contain abundant clay minerals and pyrite; thus the total weak field susceptibility is the sum of the ferromagnetic susceptibility of magnetite plus the paramagnetic susceptibility of clays and pyrite. Because paramagnetic susceptibility is a linear function in a continuous applied field, we can calculate the weak field ferromagnetic susceptibility for the 17 samples by subtracting the paramagnetic contribution. The measured weak field susceptibilities vary from 50 to 100 ($x10^{-9}$) m^3/kg with uncertainties of about 5%. Paramagnetic susceptibilities vary from 30 to 100 ($x10^{-9}$) m^3/kg with uncertainties of 2%. The similar susceptibilities of the two contributing components account for very large uncertainties on the calculated ferromagnetic susceptibilities, which can be more than 100%. For this reason, when the weak field susceptibilities are plotted against anhysteretic susceptibilities (Figure 3a), the interpretation is ambiguous. Figure 3a, however, clearly shows two populations. Most of the samples with weak ARMs fall in the multidomain-grain region between 1 and 20 μm, while the samples with strong ARMs fall in the field of pseudo single or single-domain grains [*King et al.*, 1982; 1983]. Interestingly, the SEM observations show that coarse grains (between 2 to 30 μm) of detrital magnetite/titanomagnetite exist in all samples; however, fine-grained magnetite (0.3 to 2 μm) is only abundant in carbonate-rich samples. It is likely that magnetite exists in much finer grain sizes, which could not be resolved by direct observation. Hence microscopic observations are in good agreement with the magnetic data, suggesting that the weak ARM values are the result of a magnetite mineral assemblage dominated by coarse grains, while the strong ARM values are the result of the dominance of fine grains. When samples with the strongest ARM values are also carbonate rich, there is even a greater chance that they will possess very fine-grained magnetite.

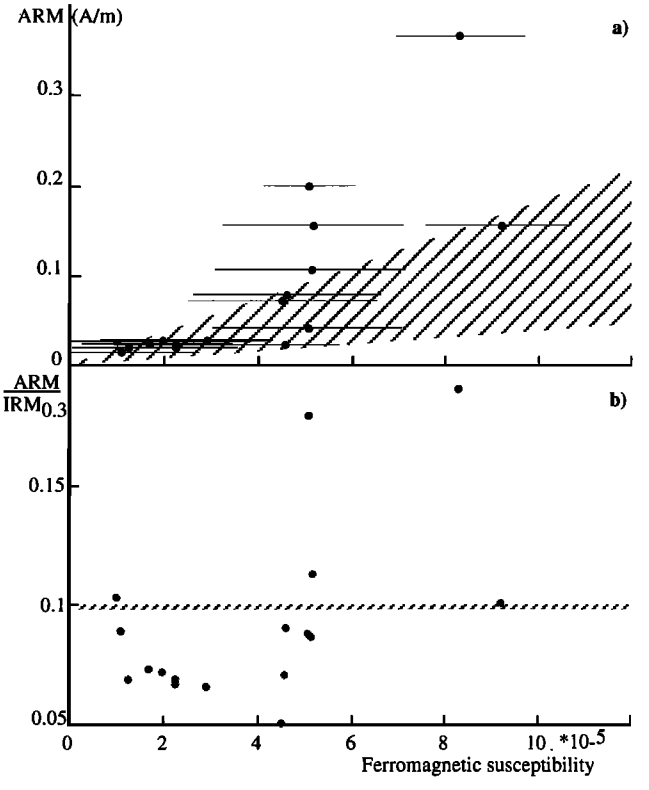

Figure 3. Estimation of magnetite grain size. (a) ARM versus the weak field ferromagnetic susceptibility calculated by subtracting the paramagnetic fraction of the total bulk susceptibility. Errors on ferromagnetic susceptibility can exceed 100%, (b) $ARM/IRM_{0\,3}$ versus ferromagnetic susceptibility. Note that samples with a magnetite mineral assemblage dominated by fine grains have $ARM/IRM_{0\,3} > 0.1$.

One criterion to estimate grain size is the ARM/IRM ratio, which according to *Özdemir and Banerjee* [1982] and *King et al.* [1983], decreases as the grain size increases up to 0.01-10 μm, then increases when the grain size varies between 20 and 100 μm. This criterion appears suitable for this study, since as shown in Figure 3a and by SEM observations, very large (>30 μm) magnetite grains are absent. The IRM signal comes from both magnetite and hematite. In a field of 0.3 T the contribution of hematite is weak, whereas the magnetite is saturated and therefore at its maximum value. In order to eliminate the magnetic contribution of hematite, we based our grain size interpretations on the $ARM/IRM_{0\,3}$ ratio ($IRM_{0\,3}$ being IRM acquired in a field of 0.3 T) which is independent of hematite. Figure 3b shows ARM/ $IRM_{0\,3}$ ratios plotted versus weak field susceptibility. The samples with magnetite mineral assemblages dominated by coarse grains have ARM/ $IRM_{0\,3}$ ratios between 0.05 and 0.1, while those dominated by fine grains have ARM/ $IRM_{0\,3}$ ratios higher than 0.1. We think that an ARM/ $IRM_{0\,3}$ value of 0.1 is suitable to distinguish between coarse and fine-grained magnetite assemblages.

3.4. Geochemical Study and Correlation With Magnetic Data.

Ader and Javoy [1998] measured the percentage of organic carbon (Corg%), the percentage of calcite, and the $\delta^{13}C$ of the bulk calcite in the Montcornet samples from this particular interval. Analytical techniques and results obtained for these

three parameters are briefly presented here. For the analysis of organic carbon, powdered carbonate samples were first dissolved in HCl. After washing four times in distilled water, the residue was combusted in a sealed tube, and then the liberated CO_2 was purified and quantified in a vacuum line. For calcite analyses the powdered samples were reacted under vacuum with 100% phosphoric acid at 25°C [*McCrea*, 1950]. The liberated CO_2 was purified and quantified in a vacuum line and analyzed for its carbon isotopic composition on a Finnigan Mat Delta E mass spectrometer. The results are reported in the usual delta notation "δ" relative to the international carbon standard Pee Dee Belemnite (PDB). Reproducibility is 0.05‰.

Calcite content in the section varies between 67% and 7% on a decimeter to meter length scale (Figure 1d). The organic carbon content decreases from 1.7 to 0.3% with increasing calcite content (Figure 4a), and $\delta^{13}C$ increases from -3‰ to +0‰ with increasing calcite content (Figure 4b): for 7%<$CaCO_3$<20%, $\delta^{13}C$ increases sharply with calcite content (-3.1<$\delta^{13}C$ <-0.7‰), for 20%< $CaCO_3$<30% there is a transition zone where $\delta^{13}C$ is spread between -1.5 and -0.2‰. The $\delta^{13}C$ is relatively constant around 0‰ for $CaCO_3$>30%.

ARM and IRM typically decrease as the quantity of $CaCO_3$ increases. We investigated the relationships between ARM, IRM, $ARM/IRM_{0.3}$, and both the $\delta^{13}C$ and the percentage of $CaCO_3$. ARM and IRM versus $CaCO_3$ show a high degree of scatter (Figures 5a and 5b). Samples rich in calcite have $ARM/IRM_{0.3}$ ratios greater than 0.1 (Figure 6). $ARM/IRM_{0.3}$ versus $\delta^{13}C$ (Figure 7) clearly shows two trends: if $\delta^{13}C$ is lower than -0.5‰, the $ARM/IRM_{0.3}$ ratio is lower than 0.1, and if $\delta^{13}C$ is above -0.5‰, the $ARM/IRM_{0.3}$ ratio varies up to 0.3. It is interesting to note those ARM/IRM0.3 values higher than 0.1 are very well grouped in $\delta^{13}C$ space, whereas they are dispersed in $CaCO_3$ space (Figure 6).

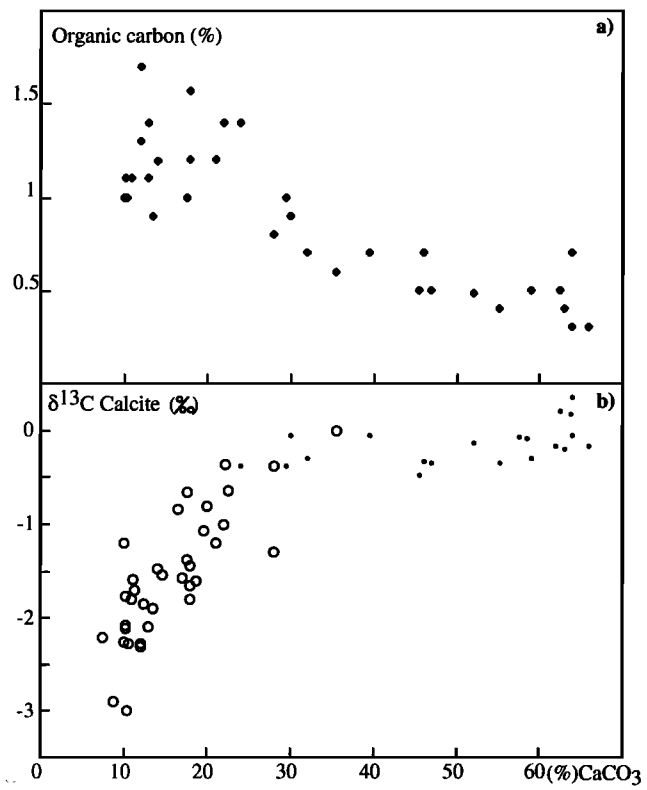

Figure 4. Variations in carbonate content versus (a) organic carbon and (b) bulk calcite $\delta^{13}C$. Small solid dots represent samples with fine-grained magnetite, and open circles represent samples with coarse-grained magnetite.

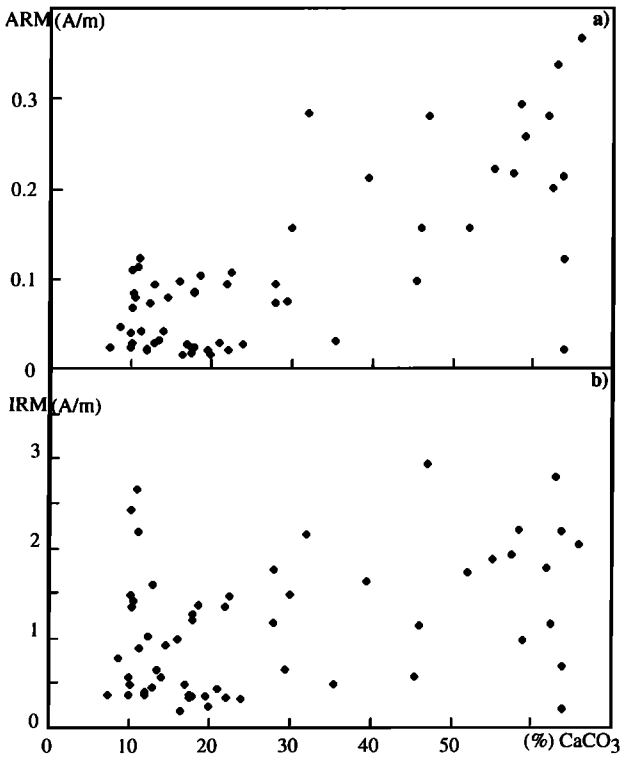

Figure 5. Variations in carbonate content versus (a) ARM and (b) IRM.

If one interprets the $ARM/IRM_{0.3}$ variations in terms of grain size, then samples with $\delta^{13}C$<-0.5‰ correspond to magnetite assemblages dominated by coarse grains. On the contrary, when $\delta^{13}C$ approaches zero, fine-grained magnetite assemblages dominate, except for three samples in which coarse-grained magnetite is probably dominant. One sample (1049.82) has $ARM/IRM_{0.3}$ ratios > 0.1 where $\delta^{13}C$ is -1.7‰ (Figure 7). We studied this sample in more detail. It contains a burrow filled with a mixed magnetite assemblage dominated by fine grains, while the rest of the sample, used for the geochemical analysis, contained coarse-grained magnetite. This sample was therefore omitted from further consideration.

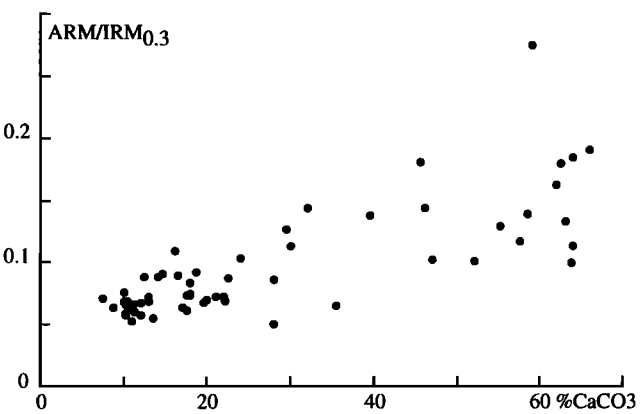

Figure 6. $ARM/IRM_{0.3}$ versus carbonate content.

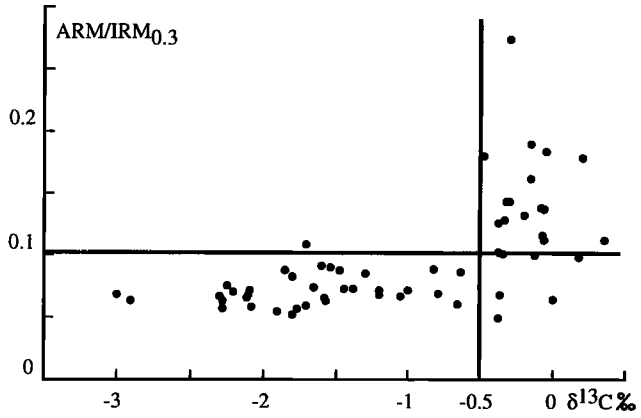

Figure 7. ARM/IRM$_{0\,3}$ versus $\delta^{13}C$. The diagram clearly shows a limit that when $\delta^{13}C < -0.5‰$ and ARM/IRM$_{0\,3} < 0.1$.

The values plotted on Figure 4b are divided into two populations; small solid dots represent fine-grained magnetite (ARM/ IRM$_{0\,3}$> 0.1) and open circles represent coarse-grained magnetite (ARM/IRM$_{0\,3}$<0.1). The ARM/IRM$_{0\,3}$ ratio effectively demarcates the two trends in Figure 4b. For the zone $CaCO_3$ >35% and $\delta^{13}C \approx 0‰$, the magnetite is essentially fine-grained; when $CaCO_3$<20%, the magnetite is coarse-grained. For the zone 20%< $CaCO_3$<35%, magnetite can be either fine or coarse-grained.

4. Interpretation

Microscopic observations show that coarse detrital grains reside in clay-rich samples, whereas fine detrital grains reside in more carbonate-rich samples. For calcite-rich samples, both the SEM observation of diffuse iron in calcite grains and large ARM/IRM$_{0\,3}$ values suggest the presence of very fine grains. It is possible that biogenic magnetite (magnetosomes) formed in these sediments. For example, in recent deep-sea sediments from the North Atlantic Ocean, *Schwartz et al.* [1997] showed that bacterial magnetosomes are abundant in calcite-rich sediments; however, it was not clear if the biomagnetite was restricted to calcite-rich zones or if the biomagnetite was dissolved elsewhere. *Schwartz et al.* [1997] noted that the magnetosomes were absent when the clastic content was high or the organic matter content was low. In the Montcornet section, organic matter typically decreases as the quantity of $CaCO_3$ increases (Figure 4a). Thus it seems quite likely that biomagnetite grains were present in all of the samples before the iron was reduced [*Karlin et al.*, 1987].

Magnetite dissolution can be important in calcite-poor samples as evidenced by the etching of grains and the low proportion of fine (0.5-5 μm) grains. On the contrary, in calcite-rich samples, evidence for dissolution is not obvious and fine magnetite grains (0.5-5 μm) are common. According to *Canfield and Berner* [1987], dissolution of magnetite depends on three parameters: (1) the H_2S concentration, (2) the specific surface area of magnetite (small grains are dissolved first), and (3) the time that H_2S is in contact with magnetite. Magnetite dissolution occurs during early diagenesis, at the same time as sulfate reduction, and after more reactive iron oxides have been reduced to pyrite [*Canfield et al.*, 1992]. The dissolution of magnetite grains in carbonate-poor samples indicates a relatively high concentration of H_2S in interstitial pore water. On the contrary, the presence of fine magnetite grains in carbonate-rich samples indicates that the H_2S concentration was insufficient to dissolve them.

The inferred mechanism accounting for the $\delta^{13}C$ variations is dissolution-precipitation of calcite out of an isotopically light interstitial fluid [*Ader and Javoy*, 1998]. The mineralization of organic matter produces low $\delta^{13}C$ (around –26‰) dissolved inorganic carbon and induces the dissolution of primary calcite (around 0‰). Sulfate reduction produces HS^-, which induces the precipitation of pyrite if the Fe content is high enough. In turn, if the precipitation of pyrite increases the pore fluid alkalinity

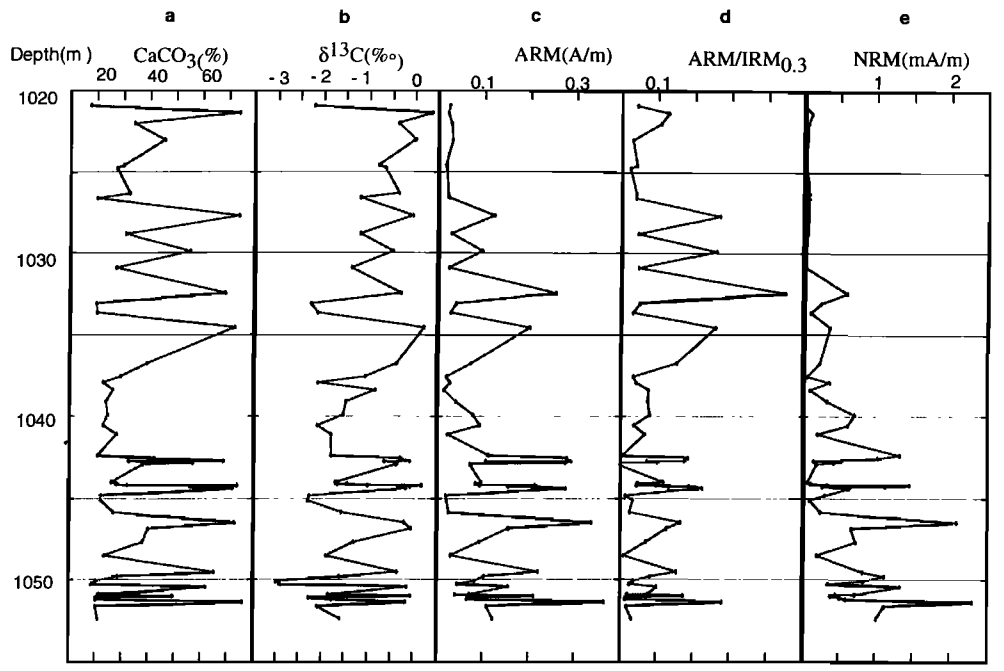

Figure 8. Depth variations for studied samples versus (a) calcite content, (b) $\delta^{13}C$, (c) ARM, (d) ARM/IRM$_{0\,3}$, and (e) NRM intensity after 300°C cleaning.

enough, secondary calcite can precipitate from the low $\delta^{13}C$ dissolved inorganic carbon. Two interpretations can account for the $\delta^{13}C$ variations of Montcornet samples. The first is that diagenesis occurred differently in calcite-poor and calcite-rich samples. Sulfate reduction was stronger in the calcite-poor samples ($\delta^{13}C$<-0.5‰), due to the higher Fe contents, and/or higher fluid confinement. The second possibility is that the sulfate reduction occurred similarly in both calcite-poor and calcite-rich samples. The relation between $\delta^{13}C$ and $CaCO_3$ (Figure 4b) would then be a mixing relation between primary and secondary calcite. However, this second hypothesis can be ruled out by the SEM observations and magnetic data because magnetite was affected quite differently by sulfate reduction in calcite-rich and calcite-poor samples. In a similar way, (1) correlations between $\delta^{13}C$, $\delta^{18}O$, and the bulk calcite content, (2) low $\delta^{13}C$ of calcite-poor samples not explained by a primary origin [*Land*, 1989; *Renard*, 1986], and (3) recrystallized bioclasts and framboïdale pyrite are easily explained by a diagenetic mechanism linked to sulfate reduction [*Ader and Javoy*, 1998].

In conclusion, both the magnetic and isotopic data suggest that the calcite-rich samples were not modified by sulfate reduction during diagenesis. Calcite-rich samples have $\delta^{13}C$ close to zero and strong ARMs and likely contain primary magnetite which may be of biogenic origin. Calcite-poor samples have been strongly modified by sulfate reduction during diagenesis. They have negative $\delta^{13}C$ and weak ARMs, suggesting that the fine magnetite grains were dissolved, leaving behind only large grains. We note two alternatives for this general rule between the limestones and claystones: either the sulfate reduction activity was weaker in limestones than in claystones, or the limestones are more permeable and do not allow the H_2S concentration to increase until the primary magnetite is dissolved.

5. Implications for Magnetostratigraphy

The calcite content, $\delta^{13}C$, ARM, $ARM/IRM_{0\,3}$, and NRM intensity (after cleaning at 300° C), are plotted versus depth on Figure 8. The variations in geochemical and rock-magnetic parameters are quite well synchronized. The NRM intensity does not mimic all the variations of the other parameters because it also depends on the intensity of the magnetic field at the time of magnetization. In order to understand the link between rock magnetism and the magnetic field record, we plotted NRM intensity versus the concentration of $CaCO_3$ (Figure 9). Magnetite grain size is indicated by differing symbols. For $CaCO_3$ < 20% the magnetite is coarse-grained, and the NRM intensities vary from 0.01 to 1.5 mA/m, with the strongest values given by the samples with the lowest calcite content. For 20%< $CaCO_3$<30%, we have already noted that magnetite can be fine- or coarse-grained. For four coarse-grained samples the NRM intensity is stronger than expected given their $CaCO_3$ concentrations. For these samples, there is likely a mix of fine and coarse magnetite grains. For $CaCO_3$>30% the magnetite is essentially fine-grained. NRM intensity varies from 0.01 to 2.5 mA/m, with the strongest values corresponding to the samples richest in $CaCO_3$. If this fine-grained magnetite is biogenic, then biogenic magnetite is an effective contributor to the NRM intensity in calcite rich-zones. These observations are complementary to those of *Schwartz et al.* [1997].

5.1.Acquisition of Magnetization

The sedimentary rocks from the Montcornet section separate into two groups. Most calcite-rich zones have not been modified by diagenesis, whereas the clay-rich zones have been. For most calcareous zones the magnetization is carried by fine-grained magnetite that can be either primary or authigenic. *Karlin* [1987] thinks that bacterial magnetite formation is restricted to a zone between nitrate and iron reduction levels. If true, then the magnetization was probably acquired soon after deposition, and the remanence within calcareous zones is reliable. For the clay-rich zones, as the small grains were preferentially dissolved, only the coarser grains remained, and the lock-in remanence of the large grains was probably rapid [*Channel*, 1978]. In all cases the acquisition of magnetization was rapid and essentially simultaneous with sedimentation. We note that in reducing sediment, hematite is probably primary, and its magnetization is also acquired soon after deposition.

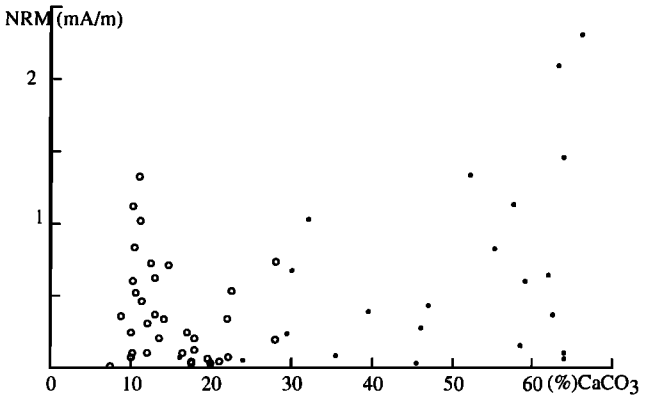

Figure 9. NRM intensity after 300°C cleaning versus carbonate content. Small solid dots represent fine-grained magnetite, and open circles represent coarse-grained magnetite.

5.2. Implications for Magnetostratigraphy

It is well known that single-domain magnetite is a better recorder than multidomain magnetite. Domain wall migration causes large grains to more readily acquire a viscous magnetization. Thus the NRM of the largest grains tends to be viscous, and zones containing only large magnetite grains will tend to be remagnetized by the ambient magnetic field. In the extreme cases these zones are void of steady remanent magnetizations.

For Montcornet, *Yang et al.* [1996], showed that the magnetic direction that defines the present dipole field is isolated by heating to 300°C. In samples from very clay-rich zones, where the small grains have disappeared, the remaining primary magnetization is carried by the large pseudo-single domain or multidomain grains. This primary magnetization is characterized by weak intensities and is more resistant to alternating field demagnetization. In magnetostratigraphic studies, one sample is sufficient to define a polarity change. However, if no fine magnetic grains are present to preserve the primary signal, the reversal may not be recorded, whereas the recording of the geomagnetic signal is enhanced when the sediment has fine-grained magnetite (as for carbonate-rich samples). For example, sample 1028.72 was rejected by *Yang et al.* [1996] because they did not succeed in segregating the viscous magnetization from the characteristic magnetization. The sample just below (1028.75) shows a reversed polarity and suggests that at this level, the authors may have missed a short normal polarity event, due to the absence of fine-grained magnetite. Thus for the studied zone between 1020 and 1052 m, it is possible that one polarity event was missed. For the total magnetostratigraphic

section, such uncertainties are scarce because the sampling density was increased in cases where the polarity was poorly defined. For instance, in two cases around 1070 m, the polarity was assigned as reversed based on three successive samples which showed a tendency toward reverse polarity. Sample by sample reexamination of the entire Montcornet core section [*Yang et al.*, 1996] now sheds doubt on the polarity designation of sample 994.32, which is normal, sandwiched between two reversed polarity neighbors (994.22 and 994.42). No other doubtful cases such as this one have been identified.

6. Conclusion

One purpose of this study was to confirm the Jurassic magnetostratigraphy proposed by *Yang et al.* [1996]. To do so, we studied the rock magnetic and geochemical properties of the rocks that would provide information about diagenetic reactions and their consequences for magnetization in claystone-limestone successions. When samples are rich in carbonate, the primary signal is well preserved. When the $CaCO_3$ content is lower than 30%, chemical modification of the pore fluids by sulfate reduction disturbs the primary signal. Mineralization of organic matter together with sulfate reduction produces H_2S and dissolves inorganic carbon with low $\delta^{13}C$. H_2S in high enough concentrations dissolves fine-grained magnetite and precipitates pyrite, which facilitates the crystallization of secondary carbonate with low $\delta^{13}C$.

At the same time that $\delta^{13}C$ is disturbed, all the fine magnetite grains are dissolved. The dissolution of large grains follows more complex laws. Magnetite with variable grain sizes is not suitable for studies concerning intensity variations of the ancient magnetic field. However, because the iron liberated from the dissolved magnetite will precipitate in the form of paramagnetic pyrite, paleomagnetic directions will be preserved. In these cases, both the paleomagnetic data and their magnetostratigraphic implications are reliable.

Finally, many discussions have centered on the impact of bacterial magnetite in preservation of stable magnetizations. If biomagnetite grows in sediment relatively poor in organic matter, the magnetite should be preserved and should record the field at the time of precipitation. If, on the other hand, biomagnetite grows in sediment rich in organic matter, the magnetite grains will be dissolved during iron reduction directly after precipitation. In such cases, the contribution of these grains to paleomagnetism is negligible.

Acknowledgments. This research was supported by the Laboratoire de Paléomagnétisme and the Laboratoire de Géochimie des Isotopes Stables at the Institut de Physique du Globe of Paris. S. Gilder contributed by useful comments on earlier versions of the manuscript. M. Schwartz, F. Lévêque, an anonymous reviewer, and M. Prévot formally reviewed the manuscript. Help from P.Weiler for improvement of the English is also much appreciated This is IPGP contribution 1633.

References

Ader , M., and M. Javoy, Diagenèse en milieu sulfuré réducteur· une étude isotopique dans le Jurassique basal du Bassin Parisien, *C.R. Acad Sci. Paris, 327*,803-809, 1998.

Canfield , D., and R. Berner, Dissolution and pyritization of magnetite in anoxic marine sediments, *Geochim. Cosmochim. Acta, 51*, 645-659, 1987.

Canfield, D., R Raiswell, and S. Bottrell, The reactivity of sedimentary minerals toward sulfide, *Am. J. Sci., 292*, 659-683, 1992.

Channel, J. E. T., Dual magnetic polarity measured in a single bed of Cretaceous palegic limestone from Sicily, *J. Geophys., 44*, 613-622, 1978.

Channel, J. E. T, and T. Hawthorne, Progressive dissolution of titanomagnetites at ODP Site 653 (Tyrrhenian Sea), *Earth Planet. Sci. Lett., 96*, 469-480, 1990.

Collinson, D. W., Depositional remanent magnetization in sediments, *J. Geophys. Res., 70*, 4663-4668, 1965.

Dunlop, D.J., and Ö. Özdemir, *Rock Magnetism: Fundamentals and Frontiers*, edited by D. Edwards, 573pp., Cambridge Univ. Press, New York, 1997.

Irving, E., and A. Major, Post-depositional detritical remanent magnetisation in synthetic sediment, *Sedimentology, 3*, 135-143, 1964.

Karlin, R., Magnetic mineral diagenesis in suboxic sediments at Bettis site W-N, NE Pacific Ocean, *J. Geophys. Res., 95*, 4421-4436, 1990.

Karlin, R., L. Mitchell, and G.R. Heath, Authigenic magnetite formation in suboxic marine sediments, *Nature, 326*, 490-493, 1987.

Kent, D. V., Post-depositional remanent magnetisation in deep-sea sediment, *Nature, 299*, 538-539, 1973.

King, J., S. K. Banerjee, J. Marvin, and Ö. Özdemir, A comparison of different magnetic methods for determining the relative grain size of magnetite in natural materials· Some results from lake sediments, *Earth Planet. Sci. Lett., 59*, 404-419, 1982

King, J., S. K. Banerjee, and J. Marvin, A new rock-magnetic approach to selecting sediments for geomagnetic paleointensity studies: Application to paleointensity for the last 4000 years, *J. Geophys. Res., 88*, 5911-5921, 1983.

Land, L., The carbon and oxygen isotopic chemistry of surficial Holocene marine carbonate sediment and Quaternary limestone and dolomite, in Fritz P. and J.C. Fontes, *Handbook of Environmental Isotope Geochemistry: The Marine Environment*, pp. 191-217, edited by Elsevier Sci., New York, 1989.

Leslie, B , S. Lund, and D. E. Hammond, Rock Magnetic evidence for the dissolution and authigenic growth of magnetic minerals within anoxic marine sediments of the California continental borderland, *J. Geophys. Res., 95*, 4437-4452, 1990.

Lowrie, W., Identification of ferromagnetic minerals in a rock by coercivity and unblocking temperature properties, *Geophys. Res. Lett., 17*, 159-162, 1990.

Lund, S. P., and R. Karlin, Introduction to the special section on physical and biogeochemical processes responsible for the magnetization of sediments, *J. Geophys. Res., 95*, 4353-4354, 1990.

McCrea, J.M., On the isotope chemistry of carbonates and paleotemperature scale, *J. Chem. Phys , 18*, 849-857, 1950.

McNish, A. G., and E. A. Johnson, Magnetization of unmetamorphosed varves and marine sediments, *J. Geophys. Res , 43*, 401-407, 1938.

Özdemir, Ö., and S. K. Banerjee, A preliminary magnetic study of soil samples from west-central Minnesota, *Earth Planet. Sci Lett., 59*, 393-403, 1982.

Renard, M., Pelagic carbonate stratigraphy (Sr, Mg, ^{18}O, ^{13}C), *Mar. Micropaleontol., 10*, 117-164, 1986.

Schwartz, M., S. Lund, and T.C. Johnson, Environmental factors as complicating influences in the recovery of quantitative geomagnetic-field paleointensity estimates from sediments, *Geophys. Res. Lett., 23*, 2693-2696, 1996.

Schwartz, M., S. Lund, D. Hammond, R. Schwartz, and K Wong, Early sediment diagenesis on the Blake/Bahamas Outer Ridge, North Atlantic Ocean, and its effects on sediment magnetism, *J. Geophys. Res., 102*, 7903-7914, 1997

van Hoof, A A M , and C. G. Langereis, Reversal records in marine marls and delayed acquisition of remanent magnetization, *Nature, 351*, 223-225, 1991.

Yang, Z , M G Moreau, H. Bucher, J.-L. Dommergues, and A. Trouiller, Hettangian and Sinemurian magnetostratigraphy from Paris basin, *J. Geophys. Res., 101*, 8025-8042, 1996

M. Ader and M.G. Moreau, Institut de Physique du Globe, 4 Place Jussieu, 75252 Paris cedex 05, France. (e-mail: moreau@ipgp.jussieu.fr)

(Received July 16, 1998; revised August 25, 1999, accepted September 7, 1999.)